JAERI-M
86-115

NUMERICAL STUDY OF THE ELECTRON HEATING AND CURRENT DRIVE BY THE FAST WAVES IN THE JFT-2M TOKAMAK PLASMA

August 1986

Takumi YAMAMOTO, Yoshihiko UESUGI, Katsumichi HOSHINO
Hisato KAWASHIMA and Hideo OHTSUKA

日本原子力研究所
Japan Atomic Energy Research Institute

ＪＦＴ－２Ｍトカマクプラズマにおける速波電子加熱及び電流駆動についての数値検討

日本原子力研究所那珂研究所核融合研究部
山本　巧・上杉　喜彦・星野　克道
川島　寿人・大塚　英男

（１９８６年７月１６日受理）

ＪＦＴ－２Ｍトカマク装置における200 MHz 帯の速波実験を検討した。電子密度 1.5 × 10^{19} m^{-3} 及び電子温度 2.5 keV 以上のプラズマでは，磁場方向の屈折率 $N_{//}$ ＝４の速波の有効な電子ランダウ減衰が期待される。さらに，電子温度19 keVの高温電子が２％含まれているプラズマに，100 kWの $N_{//}$ ＝２の速波を放射すると，８ kAのプラズマ電流駆動が期待される。

那珂研究所：〒311-02 茨城県那珂郡那珂町大字向山801-1

JAERI-M86-115

Numerical Study of the Electron Heating and Current Drive By the Fast Waves in the JFT-2M Tokamak Plasma

Takumi YAMAMOTO, Yoshihiko UESUGI, Katsumichi HOSHINO,
Hisato KAWASHIMA and Hideo OHTSUKA

Department of Thermonuclear Fusion Research
Naka Fusion Research Establishment
Japan Atomic Energy Research Institute
Naka-machi, Naka-gun, Ibaraki-ken

(Received July 16, 1986)

A 200 MHz fast wave experiment for the JET-2M tokamak is examined. Noticeable single-path electron Landau damping of the fast waves with the parallel refractive index of $N_{//} = 4$ is expected in the plasma with electron temperature more than 2.5 keV at the electron density of $n_e = 1.5 \times 10^{19} m^{-3}$. Furthermore, it is shown that 8 kA of the plasma current is driven by the fast waves with $N_{//} \simeq 2$ at $n_e = 3 \times 10^{19} m^{-3}$ in the single-path damping when 100 kW of the rf power radiates into the plasma in the presence of the hot electrons with the temperature of 19 keV and the fraction of the density of 2%.

Keywords: Fast Waves, Electron Heating, Current Drive, JFT-2M Tokamak

CONTENTS

目　　次

1. Introduction

Up to now, the lower-hybrid current drive (LHCD) experiments have been carried out on the JFT-2 and JFT-2M tokamaks in JAERI.[1]-[3] These experimental results have shown a high efficient current drive by the high-phase-velocity waves for a low electron density. On the other hand, these experiments have also shown that there exists a strong density threshold beyond which the plasma current can not be driven by the lower hybrid waves (LHW).[2] At higher operating densities, it is predicted that LHW excites parametric instabilities which divert momentum and energy of the LHW elsewhere and/or result in depletion of the power of LHW at a peripheral plasma and thus the current drive is inhibited. A good correlation between the excitation of the parametric decay instabilities and inefficient current drive has been observed.[2].

The problem of the density limit can presumably be overcome by increasing both the frequency of the LHW and the toroidal magnetic field.[4] However, since the range of allowed parallel refractive index $N_{//}$ is restricted for the plasma having large values of f_{pe}^2/f_{ce}^2, where f_{pe} and f_{ce} are the electron plasma and cyclotron frequencies, respectively, the LHW is forced to drive the skin current in high-temperature and high-density plasma like a fusion plasma.[5] Therefore, it is worthwhile considering a wave which can penetrate into the plasma core and couple to electrons effectively for a hot and dense plasma.

This goal suggests the experiment on a current drive by the fast wave (FWCD) in the frequency range of $10f_{ci} \lesssim f_0 \lesssim f_{LH}(0)$ where f_{ci} is the ion cyclotron frequency and $f_{LH}(0)$ is the maximum lower-hybrid (LH) resonance frequency in the plasma column. The fast waves in this frequency range may be absorbed mainly by electrons through Landau damping rather than by ions through the harmonic ion cyclotron damping even in high-temperature plasma. The Landau damping of the waves in the tokamak plasma is confirmed by a number of the LHCD experiments. It is also clear in the recent ion-cyclotron-range-of-frequency heating experiments that the fast waves can penetrate to high density plasma and are not suffered from the occurrence of nonlinear effects, such as excitation of the parametric instabilities, even for MW class of rf power radiations.[6] In this paper, discussions on FWCD experiment for the JFT-2M tokamak by using a 200 MHz are described.

The next section describes the accessibility and dispersion relation including imaginary part for the fast waves. The numerical calculations

on the absorption and current drive of the fast waves are shown in sections 3 and 4, respectively. Finally, section 5 summarizes the present study.

2. Accessibility and Dispersion Relation

Waves on the fast branch of the cold plasma dispersion equation would be launched from the antenna as a whistler and penetrate to densities higher than that in the LH resonance layer as a high frequency Alfven wave. We call both waves the fast wave for simplicity hereafter. If the well-known accessibility condition for LHW is met, the fast wave is converted to the LHW and fails to penetrate to higher densities. This condition is given by [7]

$$N_{//} \leq N_{//L} = (1-f^2/f_{ce}f_{ci})^{-1/2}, \text{ if } f \leq fc \text{ and} \tag{1}$$

$$N_{//L} = f_{pe}/f_{ce} + \{(1+(f_{pe}/f_{ce})^2(1-f_{ce}f_{ci}/f^2)\}^{1/2}, \text{ if } f>fc$$

with $f_c^2 = f_{pe}^2 f_{ci}/2f_{ce}\{(1+4f_{ce}^2/f_{pe}^2)^{1/2}-1)\}$ where f_{pi} is the ion plasma frequency. If Eq.(1) is not satisfied, then the fast waves penetrate to arbitrarily high densities, but the slow wave is stopped at the LH resonance layer.

A local electromagnetic wave dispersion relation can be obtained by $D(\omega, \vec{k}) = 0$ with

$$D(\omega, \vec{k}) = \begin{bmatrix} K_{xx}-N_{//}^2 & K_{xy} & N_\perp N_{//}(1+K_{xz}) \\ -K_{xy} & K_{xx} + K_{yy} - N_{//}^2 - N_\perp^2 & N_\perp N_{//} K_{yz} \\ N_\perp N_{//}(1+K_{xz}) & -N_\perp N_{//} K_{yz} & K_{zz} - N_{//}^2 \end{bmatrix}$$

where $\vec{N} = \vec{k}c/\omega$, ω and $\vec{k}$ are the wave angular frequency and wave number of the wave. The subscripts of // and $\perp$ denote components parallel and perpendicular to the magnetic field ($\vec{B} = B\vec{z}$), respectively. The K_{ij} are various elements of the hot plasma dielectric tensor.[8] The approximate cold dispersion relation for the fast waves is given by

$$N_\perp 2 = \frac{-K_{xy}^2-(N_{//}^2 - K_{xx})^2}{-K_{xy}^2/K_{zz}+N_{//}^2-K_{xx}} \tag{2}$$

with $K_{xy} \simeq i f_{pe}^2/f_{ce}f$, $K_{xx} \simeq 1-(f_{pi}^2/f^2-f_{pe}^2/f_{ce}^2)$ and $K_{zz}=1-f_{pe}^2/f^2$.

Equation (2) gives the evanescent region ($N_\perp^2 \leq 0$) between the antenna and

on the absorption and current drive of the fast waves are shown in sections 3 and 4, respectively. Finally, section 5 summarizes the present study.

2. Accessibility and Dispersion Relation

Waves on the fast branch of the cold plasma dispersion equation would be launched from the antenna as a whistler and penetrate to densities higher than that in the LH resonance layer as a high frequency Alfven wave. We call both waves the fast wave for simplicity hereafter. If the well-known accessibility condition for LHW is met, the fast wave is converted to the LHW and fails to penetrate to higher densities. This condition is given by [7]

$$N_{//} \leq N_{//L} = (1-f^2/f_{ce}f_{ci})^{-1/2}, \text{ if } f \leq fc \text{ and} \qquad (1)$$

$$N_{//L} = f_{pe}/f_{ce} + \{(1+(f_{pe}/f_{ce})^2(1-f_{ce}f_{ci}/f^2)\}^{1/2}, \text{ if } f>fc$$

with $f_c^2 = f_{pe}^2 f_{ci}/2f_{ce}\{(1+4f_{ce}^2/f_{pe}^2)^{1/2}-1)\}$ where f_{pi} is the ion plasma frequency. If Eq.(1) is not satisfied, then the fast waves penetrate to arbitrarily high densities, but the slow wave is stopped at the LH resonance layer.

A local electromagnetic wave dispersion relation can be obtained by $D(\omega, \vec{k}) = 0$ with

$$D(\omega, \vec{k}) = \begin{bmatrix} K_{xx}-N_{//}^2 & K_{xy} & N_\perp N_{//}(1+K_{xz}) \\ -K_{xy} & K_{xx} + K_{yy} - N_{//}^2 - N_\perp^2 & N_\perp N_{//} K_{yz} \\ N_\perp N_{//}(1+K_{xz}) & -N_\perp N_{//} K_{yz} & K_{zz} - N_{//}^2 \end{bmatrix}$$

where $\vec{N} = \vec{k}c/\omega$, ω and $\vec{k}$ are the wave angular frequency and wave number of the wave. The subscripts of // and $\perp$ denote components parallel and perpendicular to the magnetic field ($\vec{B} = B\,\vec{z}$), respectively. The K_{ij} are various elements of the hot plasma dielectric tensor.[8] The approximate cold dispersion relation for the fast waves is given by

$$N_\perp^2 = \frac{-K_{xy}^2-(N_{//}^2 - K_{xx})^2}{-K_{xy}^2/K_{zz}+N_{//}^2-K_{xx}} \qquad (2)$$

with $K_{xy} \simeq i f_{pe}^2/f_{ce}f$, $K_{xx} \simeq 1-(f_{pi}^2/f^2-f_{pe}^2/f_{ce}^2)$ and $K_{zz}=1-f_{pe}^2/f^2$. Equation (2) gives the evanescent region ($N_\perp^2 \leq 0$) between the antenna and

the plasma. The allowed $N_{//}$ would be estimated by the attenuation in the evanescent region extending from the antenna (x=0) to the cutoff ($x=x_c$). By using $|k_\perp(0)\, x_c| \simeq 1$ and $f_{pe}^2(x_c) = f_0 f_{ce}(N_{//}^2 - 1)$ and assuming the edge density profile to be modeled by $n_e(x) = x(\nabla n_e)_0$, we can obtain the upper bound of accessible $N_{//}$ given by [9]

$$N_{cut}^2 = 1 + \{c(\nabla n_e)_0/(2\pi f_{ce} n_{c0})\}^{2/3} \qquad (3)$$

where n_{c0} is the cut-off density defined by $f_{pe}=f_0$ and c the speed of light. The longer distance between the antenna and the cutoff makes the poorer couping of the antenna with plasma and thus the high-power rf radiation becomes more difficult.

The electron Landau damping of the fast waves in the plasma interior is given by

$$\frac{N_{xi}}{N_\perp} = G(\xi) / \{1 + (N_{//}^2 - K_{XX})(f_{ce}/f_{pe})^2\} \qquad (4)$$

with $G(\xi) = \sqrt{\pi}\xi^3 \exp(-\xi^2)$ and $\xi = c/(\sqrt{2}\, N_{//} v_e)$ where $N_{xi} = ck_i/\omega$, k_i is the imaginary part of the wave number of the fast wave, $v_e = \sqrt{T_e/m_e}$, T_e and m_e are the electron temperature and mass, respectively.

3. Numerical Calculations and Discussions

3.1 Accessibility Conditions

Figure 1 (a) shows the calculated bounds of the allowed $N_{//}$ versus the frequency at the toroidal magnetic field of B_t = 1.0 T. The solid and dotted lines in Fig. 1 (a) indicate the lower and upper bounds of $N_{//}$, $N_{//L}$ and $N_{//cut}$, respectively. The waves with $N_{//} \gtrsim 1.3$ for $f_0 \lesssim 300$ MHz can propagate in a dense plasma, while $N_{//L}$ for $f_0 \lesssim 500$ MHz increases with the density. On the other hand, $N_{//cut}$ decreases with increasing the frequency, For the high frequency, $N_{//L}$ and $N_{//cut}$ overlaps at a density that means no allowed $N_{//}$ in the peak density which is given by $n_e(0) = a(\nabla n_e)_0$. It is found out that the fast waves with $f_0 \lesssim 200$ MHz are in a good accessible region for $n_e \gtrsim 0.7 \times 10^{19}$ m^{-3} which allows $1 \sim 4$ of $N_{//}$

3.2 Slab Model

Now we consider a simple slab model in order to understand the damping of the fast waves in a wide range of the relevant parameters. The absorption efficiency in single path is given by

the plasma. The allowed $N_{//}$ would be estimated by the attenuation in the evanescent region extending from the antenna (x=0) to the cutoff ($x=x_c$). By using $|k_\perp(0)\, x_c|=1$ and $f_{pe}^2(x_c)=f_0 f_{ce}(N_{//}^2-1)$ and assuming the edge density profile to be modeled by $n_e(x)=x(\nabla n_e)_0$, we can obtain the upper bound of accessible $N_{//}$ given by [9]

$$N_{cut}^2 = 1 + \{c(\nabla n_e)_0/(2\pi f_{ce} n_{c0})\}^{2/3} \qquad (3)$$

where n_{c0} is the cut-off density defined by $f_{pe}=f_0$ and c the speed of light. The longer distance between the antenna and the cutoff makes the poorer couping of the antenna with plasma and thus the high-power rf radiation becomes more difficult.

The electron Landau damping of the fast waves in the plasma interior is given by

$$\frac{N_{xi}}{N_\perp} = G(\xi)/\{1 + (N_{//}^2 - K_{XX})(f_{ce}/f_{pe})^2\} \qquad (4)$$

with $G(\xi) = \sqrt{\pi}\xi^3 \exp(-\xi^2)$ and $\xi = c/(\sqrt{2}\, N_{//} v_e)$ where $N_{xi} = ck_i/\omega$, k_i is the imaginary part of the wave number of the fast wave, $v_e = \sqrt{T_e/m_e}$, T_e and m_e are the electron temperature and mass, respectively.

3. Numerical Calculations and Discussions

3.1 Accessibility Conditions

Figure 1 (a) shows the calculated bounds of the allowed $N_{//}$ versus the frequency at the toroidal magnetic field of B_t = 1.0 T. The solid and dotted lines in Fig. 1 (a) indicate the lower and upper bounds of $N_{//}$, $N_{//L}$ and $N_{//cut}$, respectively. The waves with $N_{//} \gtrsim 1.3$ for $f_0 \lesssim 300$ MHz can propagate in a dense plasma, while $N_{//L}$ for $f_0 \lesssim 500$ MHz increases with the density. On the other hand, $N_{//cut}$ decreases with increasing the frequency, For the high frequency, $N_{//L}$ and $N_{//cut}$ overlaps at a density that means no allowed $N_{//}$ in the peak density which is given by $n_e(0) = a(\nabla n_e)_0$. It is found out that the fast waves with $f_0 \lesssim 200$ MHz are in a good accessible region for $n_e \gtrsim 0.7 \times 10^{19}$ m^{-3} which allows $1 \sim 4$ of $N_{//}$

3.2 Slab Model

Now we consider a simple slab model in order to understand the damping of the fast waves in a wide range of the relevant parameters. The absorption efficiency in single path is given by

$$\frac{P_{ab}}{P_0} = 1 - \exp(-2\, k_i \Delta L) \qquad (5)$$

where ΔL is the length of the uniform plasma and k_i is calculated from Eq.(4). Calculated value of P_{ab}/P_0 versus the frequency as a parameter of $N_{//}$ is shown in Fig. 1 (b). The damping of the fast waves increases with the frequency because of the increase in the parallel component of the electric field. Furthermore, the high $N_{//}$ makes the strong damping for $f_0 \gtrsim 200$ MHz. The value of $N_{//} = 4$ corresponds to $c/(N_{//}v_e) = 2.6$, which is close to the optimum value in the Landau damping. Therefore, we choose 200 MHz of the fast-wave frequency as the optimum frequency on the JFT-2M tokamak taking account of the accessibility and damping of the fast waves and available frequency of the high-power triode/tetrode.

Figure 2 shows n_e-T_e diagram of the absorption efficiency for f_0=200 MHz. The high n_e and T_e lead to the high absorption efficiency. The value of $P_{ab}/P_0 \gtrsim 0.1$ requires the electron temperature of $T_e \geq 2.5$ KeV at $n_e = 1.5 \times 10^{19}$ m^{-3}, which has been achieved by electron cyclotron heating in the JET-2M tokamak.

3.3 Ray Tracing and Toroidal Effects

We study the fast wave propagation and damping in inhomogeneous plasma in a toroidal geometry, which is described to the WKB approximation by a ray tracing calculation in three dimensional model. The ray tracing computer code follows the wave trajectories by numerically integrating the following equations: [8]

$$\frac{d\vec{r}}{dt} = \frac{\partial D}{\partial \vec{k}} \Big/ \frac{\partial D}{\partial \omega}\,, \quad \frac{d\vec{k}}{dt} = \frac{\partial D}{\partial \vec{r}} \Big/ \frac{\partial D}{\partial \omega}\,. \qquad (6)$$

The conventional toroidal coordinates (r, θ, ϕ) are used with the assumption of concentric circular magnetic surfaces. ω and $\vec{k}$ satisfy the local fast wave dispersion relation, $\left| D(\omega, \vec{k}) \right| = 0$. The following JFT-2M tokamak plasma parameters are used for the present calculations:

major radius:	$R_0 = 1.31$ m
manor radius:	$a = 0.34$ m
toroidal magnetic field:	$B_t = 1.0$ T
electron density profile:	$n_e(r)/n_e(0) = \{1-(r/a)^2\}^2$
deuterium density:	$n_d(r) = n_e(r)$
electron temperature profile:	$T_e(r)/T_e(0) = \{1-(r/a)^2\}^3$

ion temperature: $T_i(r) = T_e(r)$

safety factor: $q(0) = 1.5$ (r=0)

$q(a) = 3.0$ (r=a)

safety factor profile: $q(r)/q(0) = [1-\{1-(q(0)/q(a))\}(r/a)2]^{-1}$

rf frequency: $f_0 = 200$ MHz

Figure 3 shows the calculated results for $n_e(0) = 3 \times 10^{19}$ m^{-3}, $T_e(0) = 3.0$ keV, $N_{\phi 0} = 4$ and $k_{\theta 0} = 0$. The subscript 0 denotes the initial value. The ray trajectories projected on a poloidal plane for three different start points are shown in Fig. 3(a). The numerical letters described at the beginning and end of the ray indicate the normalized rf power. All waves can reach near the plasma center and propagate outward with a damping. The waves launched from the top side, C, are damped effectively, and then $P_{ab}/P_0 = 0.46$ in the single path is obtained. On the other hand, the absorption efficiencies of the wave launched at A and B, shown in Fig. 3(a), are 0.01 and 0.37, respectively. These results are caused by the variation of $k_{//}$ along the ray trajectory, as shown in Fig. 3(b). The fast waves are mainly damped by electron Landau damping. Wave dampings via transit time magnetic pumping and harmonic ion cyclotron resonance are negligible. Most of the absorbed rf power concentrate around the plasma center. Figure 4 shows the dependence of the damping on $k_{\theta 0}$. The waves are launched from the midplane. In Fig. 4(a), the variation of $k_{//}$ along the ray trajectory for the different values of $k_{\theta 0}$ is shown. The negative sign of $k_{\theta 0}$, corresponding to the waves propagating in the direction of the poloidal magnetic field, makes the up-shift of $k_{//}$ and thus the strong Landau damping occurs. The absorption efficiency in the single path as a function of $k_{\theta 0}$ is plotted in Fig. 4(b). The result indicates that the fast waves excited by asymmetric phasing of the antenna array in the poloidal plane also favor the wave damping.

4. Current Drive by the Fast Waves

The fast waves propagating to the dense core plasma are expected to drive the plasma current efficiently for the high density by quasi-linear Landau damping. We now estimate in rough the driven plasma current. According to the numerical solution of the two-dimensional Fokker-Planck equation with an added quasi-linear term due to Landau damped waves, the normalized ratio of the current to the dissipated rf power for the ion charge state of Z_i=1 is given by [10]

ion temperature: $T_i(r) = T_e(r)$

safety factor: $q(0) = 1.5$ (r=0)

$q(a) = 3.0$ (r=a)

safety factor profile: $q(r)/q(0) = [1-\{1-(q(0)/q(a))\}(r/a)2]^{-1}$

rf frequency: $f_0 = 200$ MHz

Figure 3 shows the calculated results for $n_e(0) = 3 \times 10^{19}$ m^{-3}, $T_e(0) = 3.0$ keV, $N_{\phi 0} = 4$ and $k_{\theta 0} = 0$. The subscript 0 denotes the initial value. The ray trajectories projected on a poloidal plane for three different start points are shown in Fig. 3(a). The numerical letters described at the beginning and end of the ray indicate the normalized rf power. All waves can reach near the plasma center and propagate outward with a damping. The waves launched from the top side, C, are damped effectively, and then $P_{ab}/P_0 = 0.46$ in the single path is obtained. On the other hand, the absorption efficiencies of the wave launched at A and B, shown in Fig. 3(a), are 0.01 and 0.37, respectively. These results are caused by the variation of $k_{//}$ along the ray trajectory, as shown in Fig. 3(b). The fast waves are mainly damped by electron Landau damping. Wave dampings via transit time magnetic pumping and harmonic ion cyclotron resonance are negligible. Most of the absorbed rf power concentrate around the plasma center. Figure 4 shows the dependence of the damping on $k_{\theta 0}$. The waves are launched from the midplane. In Fig. 4(a), the variation of $k_{//}$ along the ray trajectory for the different values of $k_{\theta 0}$ is shown. The negative sign of $k_{\theta 0}$, corresponding to the waves propagating in the direction of the poloidal magnetic field, makes the up-shift of $k_{//}$ and thus the strong Landau damping occurs. The absorption efficiency in the single path as a function of $k_{\theta 0}$ is plotted in Fig. 4(b). The result indicates that the fast waves excited by asymmetric phasing of the antenna array in the poloidal plane also favor the wave damping.

4. Current Drive by the Fast Waves

The fast waves propagating to the dense core plasma are expected to drive the plasma current efficiently for the high density by quasi-linear Landau damping. We now estimate in rough the driven plasma current. According to the numerical solution of the two-dimensional Fokker-Planck equation with an added quasi-linear term due to Landau damped waves, the normalized ratio of the current to the dissipated rf power for the ion charge state of Z_i=1 is given by [10]

$$J/P_d \simeq 1.7(c/v_e)^2/\langle N_{//}^2\rangle \qquad (7)$$

where $\langle N_{//}^2\rangle = 2\log(N_1/N_2)/(N_2^{-2}-N_1^{-2})$, N_1 and N_2 are the upper and lower limits of the $N_{//}$ -spectrum of the fast waves. The numerical results also reveal that J/P_d scales 1:0.82:0.71 for Z_i=1,3 and 5.
By assuming the homogeneous plasma in the toroidal geometry and $\log\Lambda$ =15, Eq. (7) leads to

$$I_{rf} / P_{ab} = 17/\{R_0(m)\ n_e(10^{19}\ m^{-3})\ \langle N_{//}^2\rangle\}(A/W) \qquad (8)$$

where I_{rf} is the driven plasma current. It is interested that I_{rf}/P_{ab} is independent of the electron temperature, while P_{ab} strongly depends on the temperature mentioned above. When 100 kW of the fast waves with $N_{//}$=4 radiates into the plasma with T_e = 2.5 keV and n_e = 1.5 x 10^{19} m^{-3}, a 5.4 kA of the driven plasma current in single path is estimated from Eq. (8) with R_0 = 1.31 m, and $\langle N_{//}^2\rangle$=16, and P_{ab}/P_0 = 0.1 obtained from Fig. 3.

Meanwhile, Eq. (8) indicates that the fast waves with a low $N_{//}$ makes high efficiency of current drive. The fast waves with the low $N_{//}$ is unlikely to drive a number of the current in Maxwellian plasma because of a few resonant electrons coupled with the fast waves. The absorbed rf power decreases in exponential with descreasing N//. Therefore, we consider two-Maxwellians electrons in the presence of a hot electron in order to enhance the interaction between the waves and energetic electrons. The absorbed rf power is estimated from Eq. (4) in which $G(\xi)$ is replaced by $G(\xi_b) + (n_h/n_e)G(\xi_h)$ where $\xi_\ell = c/(\sqrt{2}N_{//}v_{e\ell})$ with ℓ = h or b, and h and b denote the hot and bulk components, respectively. The absorption efficiency calculated in the slab model with a uniform plasma versus n_h/n_e as a parameter of the hot electron temperature T_h is plotted in Fig. (5). We obtain P_{ab}=7 kW in the single path when 100 kW of the fast waves with $N_{//}$=2 radiates into the plasma for n_e=3 x 10^{19} m^{-3} and ΔL=0.1 m which includes the hot electrons with n_h/n_e = 2% and T_h = 19 keV. Thus the driven plasma current of 8 kA is calculated from Eq. (8) with $\langle N_{//}^2\rangle$ = 4. The hot electrons is expected to be produced by the selective electron cyclotron heating even for high density.[11] It should be noted that the absorbed rf power estimated above is not self-consistent with generation of the current. We have to solve the Fokker-Planck equation with the diffusion term due to the fast waves in order to estimate the exact absorbed rf power.

5. Summary

We examine the FWCD experiment for the JFT-2M tokamak and then choose the 200 MHz of the fast wave frequency as the optimum frequency. The numerical calculations show that the fast waves with $N_{//} = 4$ are damped appreciably by electrons via Landau damping in the plasma with $Te \geq 2.5$ keV at $n_e = 1.5 \times 10^{19}$ m^{-3}. The 100 kW launching of the fast waves with $N_{//} \simeq 2$ is expected to generate 8 kA of the plasma current in single path for the plasma at $n_e = 3.0 \times 10^{19}$ m^{-3} which includes $n_h/n_e = 2\%$ of the hot electrons with $T_h = 19$ keV.

Acknowledgements:

The authors are grateful to Drs. A. Funahashi, Y. Tanaka, M. Tanaka, and K. Tomabechi for continuous encouragements. We also thank Drs. K. Odajima and Y. Kishimoto for many helpful discussions.

References:

1. T. Yamamoto, T. Imai, M. Shimada, N. Suzuki, M. Maeno, S. Konoshima, T. Fujii, K. Uehara, T. Nagashima, and N. Fujisawa, Phys. Rev. Letters 45, 716 (1980).

2. T. Yamamoto and JFT-2 Group, in Non-Inductive Current Drive in Tokamaks (Proc. IAEA, Tech. Comittee Meeting, Culham, 1983) Vol. 1 224 (1983).

3. Y. Uesugi, K. Hoshino, T. Yamamoto, H. Kawashima, S. Kasai, T. Kawakami, M. Maeno, T. Matoba, T. Matsuda, H. Matsumoto, Y. Miura, M. Mori, K. Odajima, H. Ogawa, T. Ogawa, K. Ohta, H. Ohtsuka, S. Sengoku, T. Shoji, N. Suzuki, H. Tamai, S. Yamamoto, T. Yamauchi, and I. Yanagisawa, Nucl. Fusion 25, 1623 (1985).

4. M. Porkolob, J.J. Schuss, B. Lloyd, Y. Takase, S. Texter, P. Bonoli, C. Fiore, R. Gandy, D. Gwinn, B. Lipschultz, E. Marmar, D. Pappas, R. Parker, and P. Pribyl, Phys. Rev. Letters 53, 450 (1984).

5. K. Miyamoto, M. Sugihara, H. Kimura, H. Matsumoto, K. Odajima, T. Imai, A. Fukuyama, M. Okamoto, T. Nagashima, T. Yamamoto, T. Ohno, N. Kobayashi, T. Uchida, J. Ohmori, Y. Sawada, K. Ebisawa, K. Uchida, M. Yamauchi, and N. Fujisawa, JAERI-M 87-172 (1982).

5. Summary

We examine the FWCD experiment for the JFT-2M tokamak and then choose the 200 MHz of the fast wave frequency as the optimum frequency. The numerical calculations show that the fast waves with $N_{//} = 4$ are damped appreciably by electrons via Landau damping in the plasma with $Te \geq 2.5$ keV at $n_e = 1.5 \times 10^{19}$ m^{-3}. The 100 kW launching of the fast waves with $N_{//} \simeq 2$ is expected to generate 8 kA of the plasma current in single path for the plasma at $n_e = 3.0 \times 10^{19}$ m^{-3} which includes $n_h/n_e = 2\%$ of the hot electrons with $T_h = 19$ keV.

Acknowledgements:

The authors are grateful to Drs. A. Funahashi, Y. Tanaka, M. Tanaka, and K. Tomabechi for continuous encouragements. We also thank Drs. K. Odajima and Y. Kishimoto for many helpful discussions.

References:

1. T. Yamamoto, T. Imai, M. Shimada, N. Suzuki, M. Maeno, S. Konoshima, T. Fujii, K. Uehara, T. Nagashima, and N. Fujisawa, Phys. Rev. Letters 45, 716 (1980).

2. T. Yamamoto and JFT-2 Group, in Non-Inductive Current Drive in Tokamaks (Proc. IAEA, Tech. Comittee Meeting, Culham, 1983) Vol. 1 224 (1983).

3. Y. Uesugi, K. Hoshino, T. Yamamoto, H. Kawashima, S. Kasai, T. Kawakami, M. Maeno, T. Matoba, T. Matsuda, H. Matsumoto, Y. Miura, M. Mori, K. Odajima, H. Ogawa, T. Ogawa, K. Ohta, H. Ohtsuka, S. Sengoku, T. Shoji, N. Suzuki, H. Tamai, S. Yamamoto, T. Yamauchi, and I. Yanagisawa, Nucl. Fusion 25, 1623 (1985).

4. M. Porkolob, J.J. Schuss, B. Lloyd, Y. Takase, S. Texter, P. Bonoli, C. Fiore, R. Gandy, D. Gwinn, B. Lipschultz, E. Marmar, D. Pappas, R. Parker, and P. Pribyl, Phys. Rev. Letters 53, 450 (1984).

5. K. Miyamoto, M. Sugihara, H. Kimura, H. Matsumoto, K. Odajima, T. Imai, A. Fukuyama, M. Okamoto, T. Nagashima, T. Yamamoto, T. Ohno, N. Kobayashi, T. Uchida, J. Ohmori, Y. Sawada, K. Ebisawa, K. Uchida, M. Yamauchi, and N. Fujisawa, JAERI-M 87-172 (1982).

5. Summary

We examine the FWCD experiment for the JFT-2M tokamak and then choose the 200 MHz of the fast wave frequency as the optimum frequency. The numerical calculations show that the fast waves with $N_{//} = 4$ are damped appreciably by electrons via Landau damping in the plasma with $Te \geq 2.5$ keV at $n_e = 1.5 \times 10^{19}$ m^{-3}. The 100 kW launching of the fast waves with $N_{//} \simeq 2$ is expected to generate 8 kA of the plasma current in single path for the plasma at $n_e = 3.0 \times 10^{19}$ m^{-3} which includes $n_h/n_e = 2\%$ of the hot electrons with $T_h = 19$ keV.

Acknowledgements:

The authors are grateful to Drs. A. Funahashi, Y. Tanaka, M. Tanaka, and K. Tomabechi for continuous encouragements. We also thank Drs. K. Odajima and Y. Kishimoto for many helpful discussions.

References:

1. T. Yamamoto, T. Imai, M. Shimada, N. Suzuki, M. Maeno, S. Konoshima, T. Fujii, K. Uehara, T. Nagashima, and N. Fujisawa, Phys. Rev. Letters 45, 716 (1980).

2. T. Yamamoto and JFT-2 Group, in Non-Inductive Current Drive in Tokamaks (Proc. IAEA, Tech. Comittee Meeting, Culham, 1983) Vol. 1 224 (1983).

3. Y. Uesugi, K. Hoshino, T. Yamamoto, H. Kawashima, S. Kasai, T. Kawakami, M. Maeno, T. Matoba, T. Matsuda, H. Matsumoto, Y. Miura, M. Mori, K. Odajima, H. Ogawa, T. Ogawa, K. Ohta, H. Ohtsuka, S. Sengoku, T. Shoji, N. Suzuki, H. Tamai, S. Yamamoto, T. Yamauchi, and I. Yanagisawa, Nucl. Fusion 25, 1623 (1985).

4. M. Porkolob, J.J. Schuss, B. Lloyd, Y. Takase, S. Texter, P. Bonoli, C. Fiore, R. Gandy, D. Gwinn, B. Lipschultz, E. Marmar, D. Pappas, R. Parker, and P. Pribyl, Phys. Rev. Letters 53, 450 (1984).

5. K. Miyamoto, M. Sugihara, H. Kimura, H. Matsumoto, K. Odajima, T. Imai, A. Fukuyama, M. Okamoto, T. Nagashima, T. Yamamoto, T. Ohno, N. Kobayashi, T. Uchida, J. Ohmori, Y. Sawada, K. Ebisawa, K. Uchida, M. Yamauchi, and N. Fujisawa, JAERI-M 87-172 (1982).

6. M. Mori, K. Hasegawa, A. Honda, K. Hoshino, I. Ishibori, S. Kasai, T. Kashimura, Y. Kashiwa, T. Kawakami, H. Kawashima, M. Kazawa, M. Katagiri, K. Kikuchi, H. Kimura, Y. Koide, K. Kunieda, M. Maeno, T. Matoba, T. Matsuda, H. Matsumoto, Y. Matsuzaki, Y. Miura, H. Nakamura, I. Ochiai, K. Odajima, H. Ogawa, T. Ogawa, K. Ohota, H. Ohtsuka, K. Ohuchi, F. Okano, T. Shibata, T. Shibuya, T. Shiina, T. Shoji, K. Suzuki, N. Suzuki, H. Tamai, Y. Tanaka, T. Tani S. Tuji, Y. Uesugi, S. Yamamoto, T. Yamamoto, T. Yamauchi, I. Yanagisawa, and K. Yokoyama, in Plasma Physics and Controlled Nuclear Fusion Research 1984 (Pro. 10th Int. Conf. London 1984) Vol. 1 IAEA, Vienna, 445 (1985).

7. V.M. Glagolev, Plasma Phys. 14, 301 (1972).

8. T.H. Stix, The Theory of Plasma Wave, McGraw-Hill, New York (1962).

9. K. Ohkubo, Y. Hamada, Y. Ogawa, A. Mohri, R. Akiyama, R. Ando, S. Hirokura, E. Kako, K. Kawahata, Y. Kawasumi, K. Masai, K. Matsuoka, M. Mugishima, N. Noda, M. Sasao, K.N. Sato, S. Tanahashi, Y. Taniguchi, and K. Toi, Phys. Rev. Letters 56, 2040 (1986).

10. C.F.F. Karney and N.J. Fisch, Phys. Fluids 22,1817 (1979).

11. T. Yamamoto, K. Hoshino, Y. Uesugi, H. Kawashima, M. Mori, Y. Miura, N. Suzuki, T. Matoba, A. Funahashi, S. Kasai, T. Kawakami, T. Matsuda, H. Matsumoto, K. Odajima, H. Ogawa, T. Ogawa, H. Ohtsuka, S. Sengoku, T. Shoji, H. Tamai, T. Yamauchi, M. Hasegawa, and S. Takada, in the 13th European Conference on Controlled Fusion and Plasma Heating 1986 (to be published).

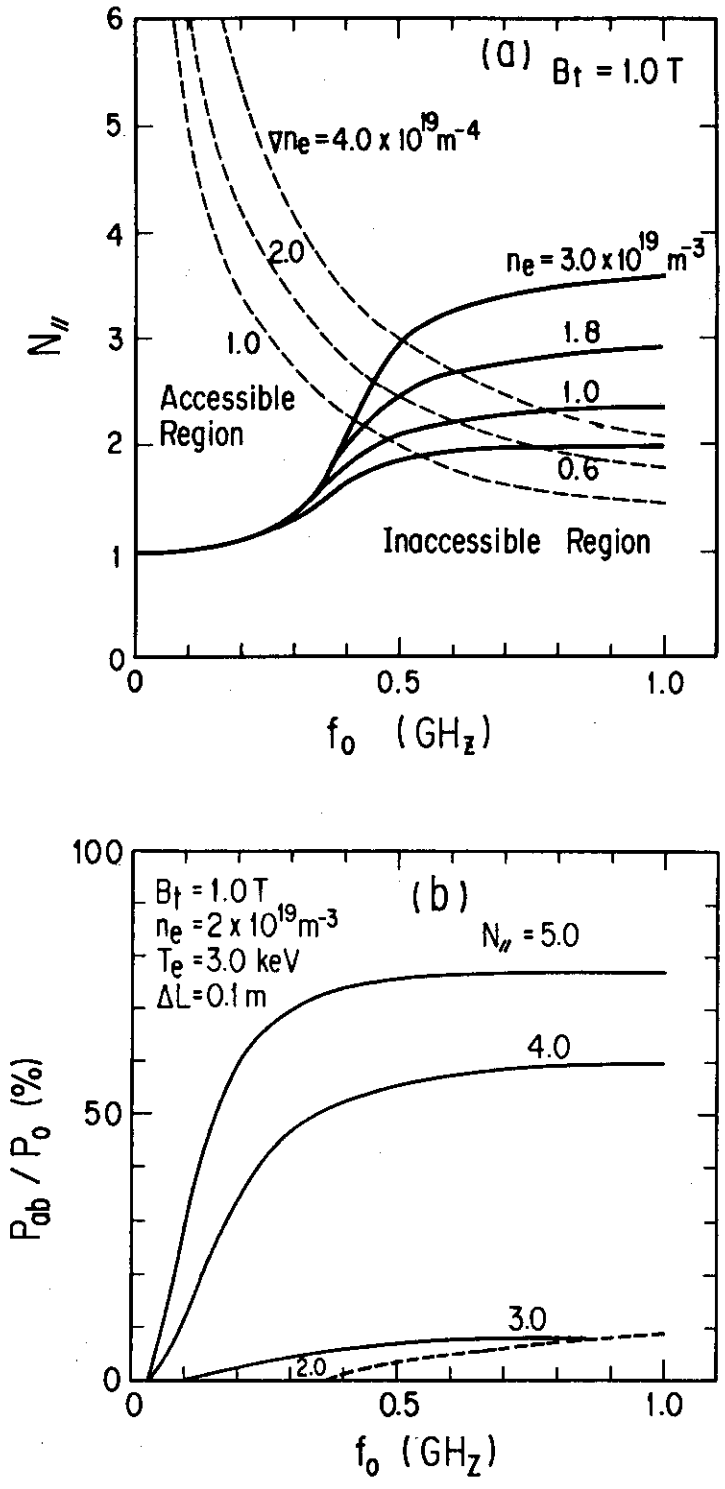

Fig.1. (a) The lower and upper bounds (the solid and dotted lines) of accessible $N_{//}$ versus the frequency of the fast waves as a parameter of electron density or density gradient, respectively. (b) Absorption efficiency P_{ab}/P_0 versus the frequency as a parameter of $N_{//}$. The dotted line indicates the lower bound of the accessible $N_{//}$ at $n_e = 2.0 \times 10^{19}$ m^{-3}.

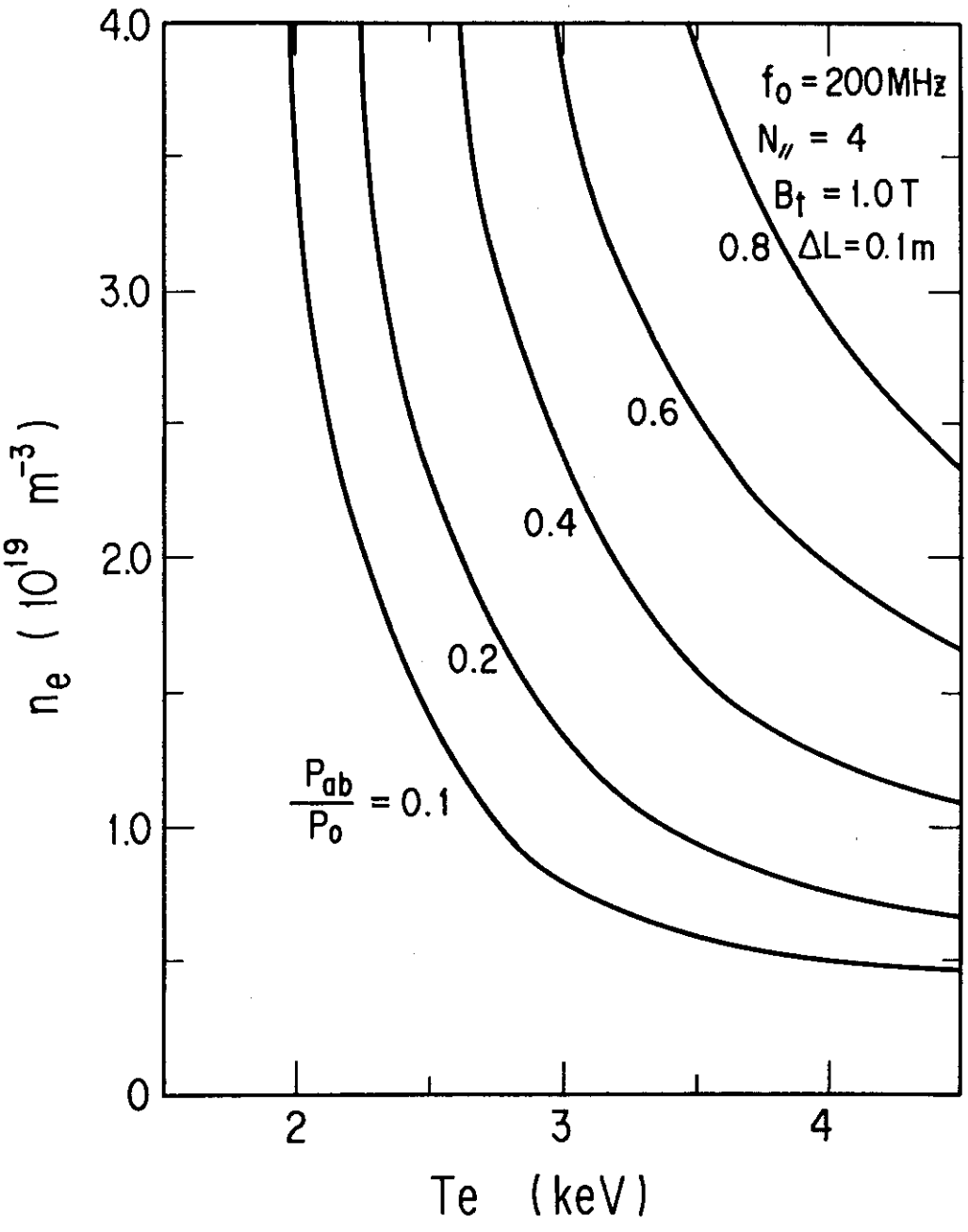

Fig. 2. Electron density and temperature diagram of the absorption efficiency calculated from the uniform slab model.

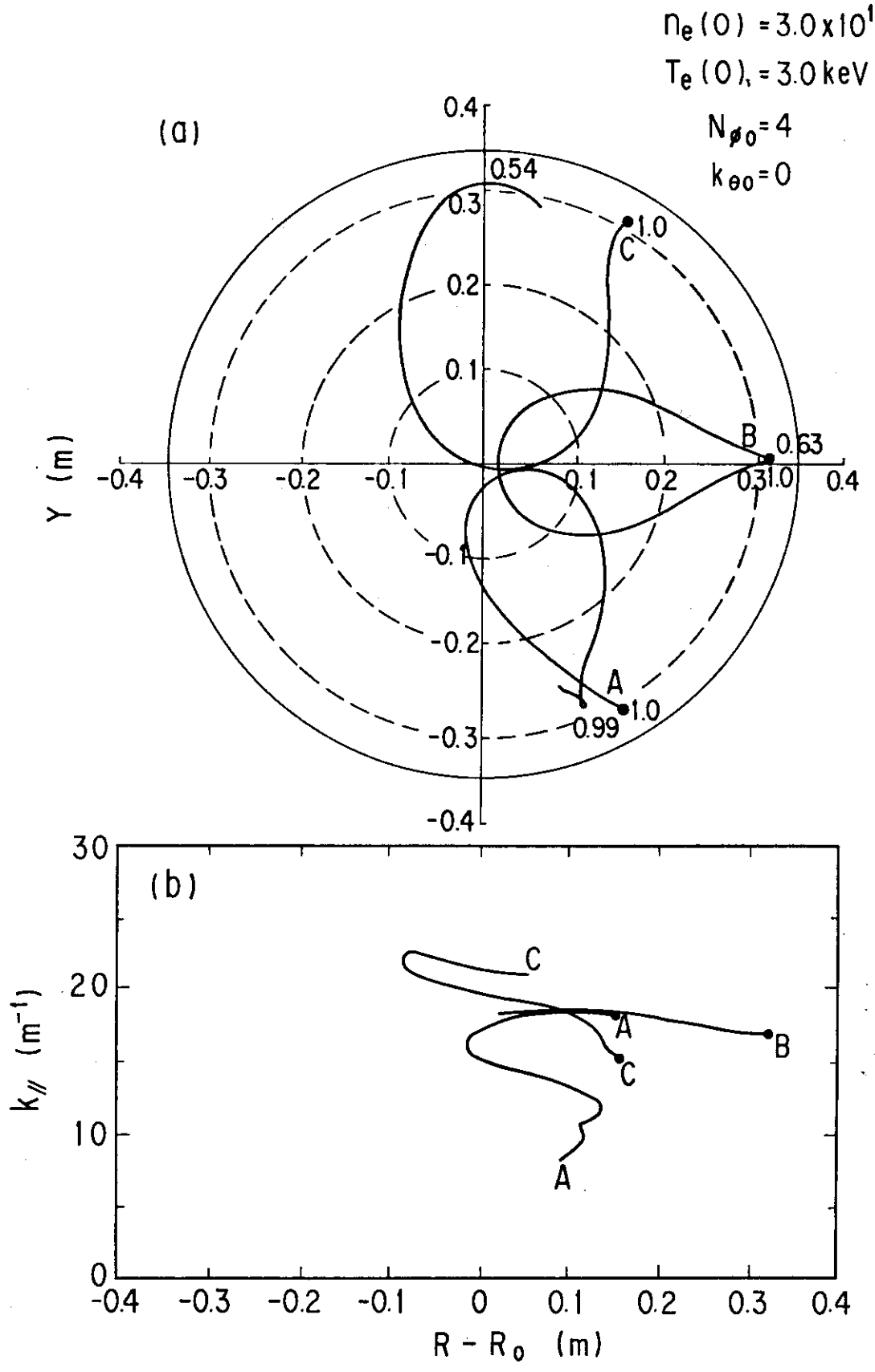

Fig.3 (a) Ray trajectories projected on the poloidal plane for three different start points, A, B, and C. f_0=200 MHz. R is the major radius. (b) Variation of $k_{//}$ along the ray trajectory. The conditions are the same as (a).

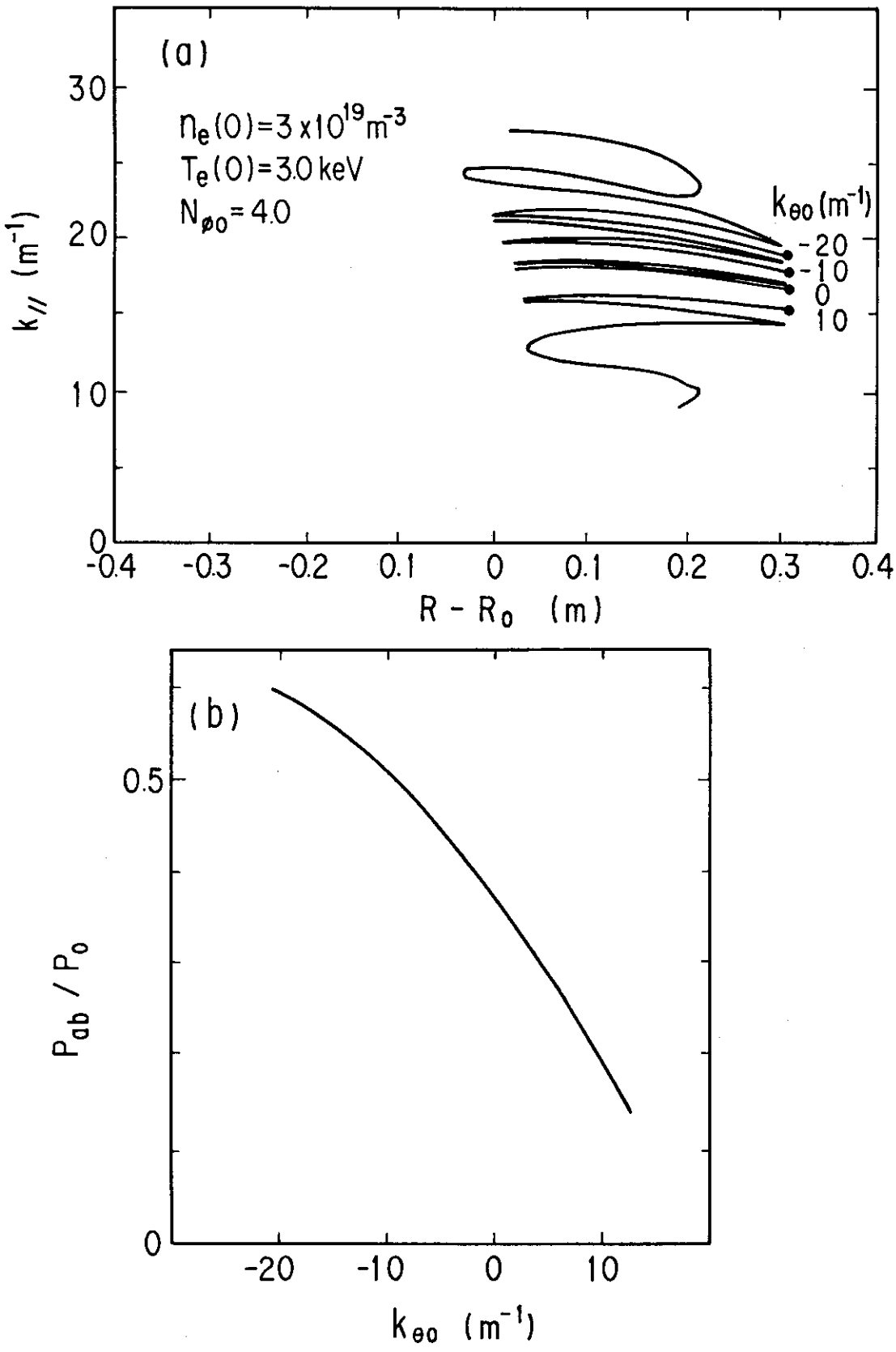

Fig.4 (a) Variation of $k_{//}$ along the ray trajectory for the different values of $k_{\theta 0}$. (b) Dependence of P_{ab}/P_{c0} in the single path on $k_{\theta 0}$. The conditions are the same as (a).

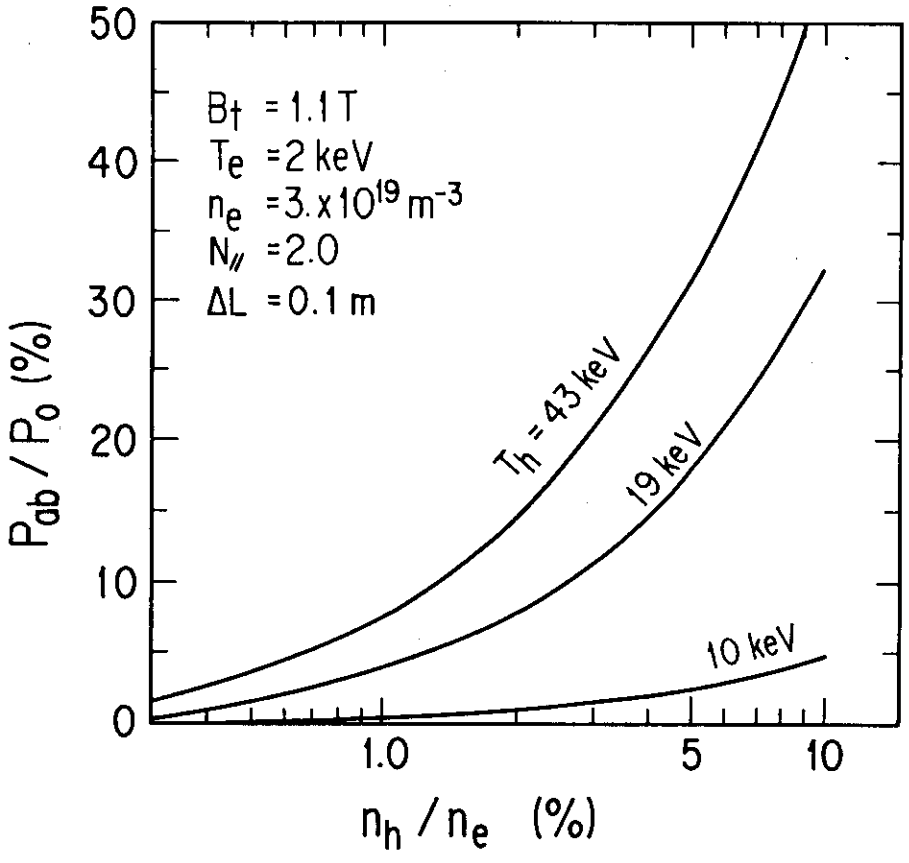

Fig.5 Absorption efficiency versus the fraction of hot electrons n_h/n_e as a parameter of the hot electron temperature T_h.